Electronic Supplementary Material (ESI) for Dalton Transactions.

Supporting Information

Design of luminescent complexes with different Cu_4I_4 cores based on pyridyl phenoxarsines

Milyausha F. Galimova,*[a] Ekaterina M. Zueva,[b] Maria M. Petrova,[b] Alexey B. Dobrynin,[a] Ilya E. Kolesnikov,[c] Elvira I. Musina,[a] Rustem R. Musin,[b] Andrey A. Karasik,[a] Oleg G. Sinyashin[a]

[a] Arbuzov Institute of Organic and Physical Chemistry, FRC Kazan Scientific Center, Russian Academy of Sciences, 8 Arbuzov Street, 420088 Kazan, Russian Federation.
E-mail: milya1949@mail.ru

[b] Kazan National Research Technological University, 68 K. Marx Street, 420015 Kazan, Russian Federation

[c] Center for Optical and Laser Materials Research, St. Petersburg University, 5 Ulianovskaya Street, 198504 Saint Petersburg, Russian Federation

Table of Contents

1. ^{1}H NMR spectra of ligands and complexes

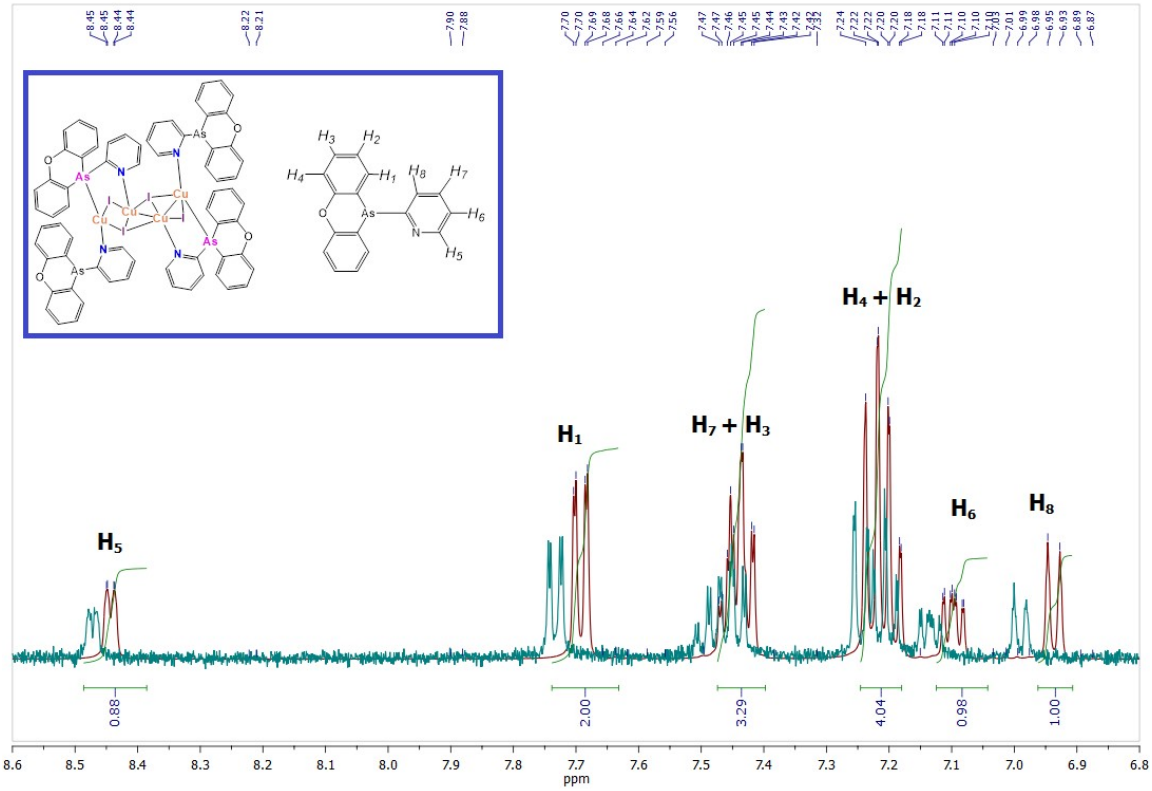

Figure S1. Comparison of ^{1}H NMR spectra for ligand **1** (red line) and complex **5** (green line) measured in CD_3CN (the range from 6.60 to 7.80 ppm is shown). The integrated intensities of NMR signals are given for red spectrum.

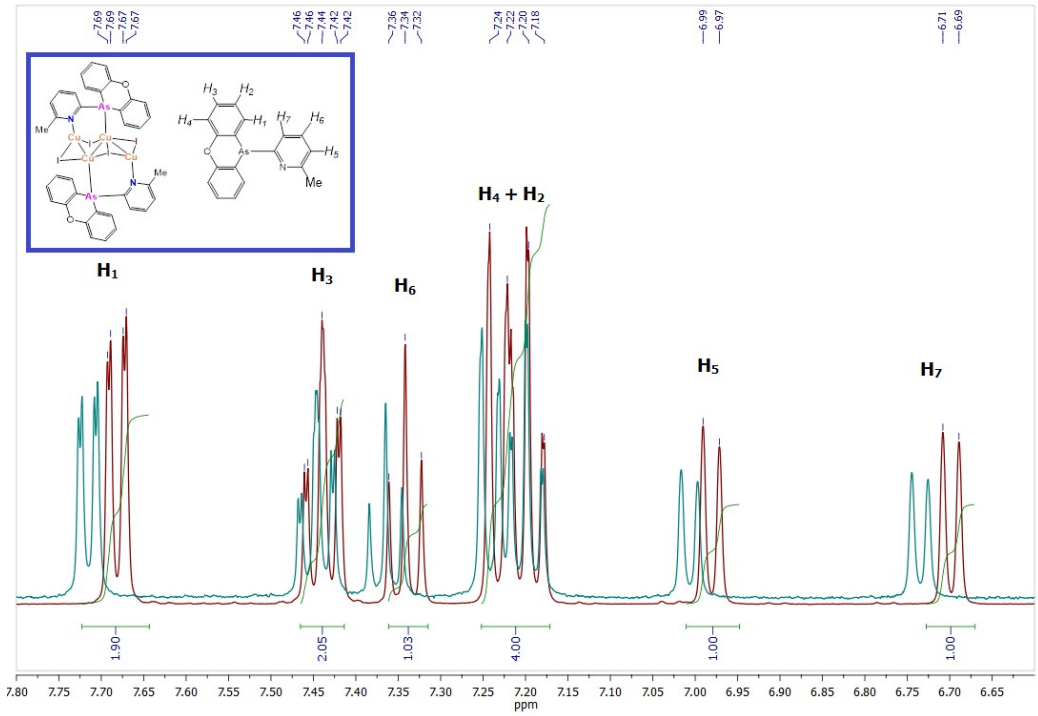

Figure S2. Comparison of ^{1}H NMR spectra for ligand **2** (red line) and complex **6** (green line) measured in CD_3CN (the range from 6.60 to 7.80 ppm is shown). The integrated intensities of NMR signals are given for red spectrum.

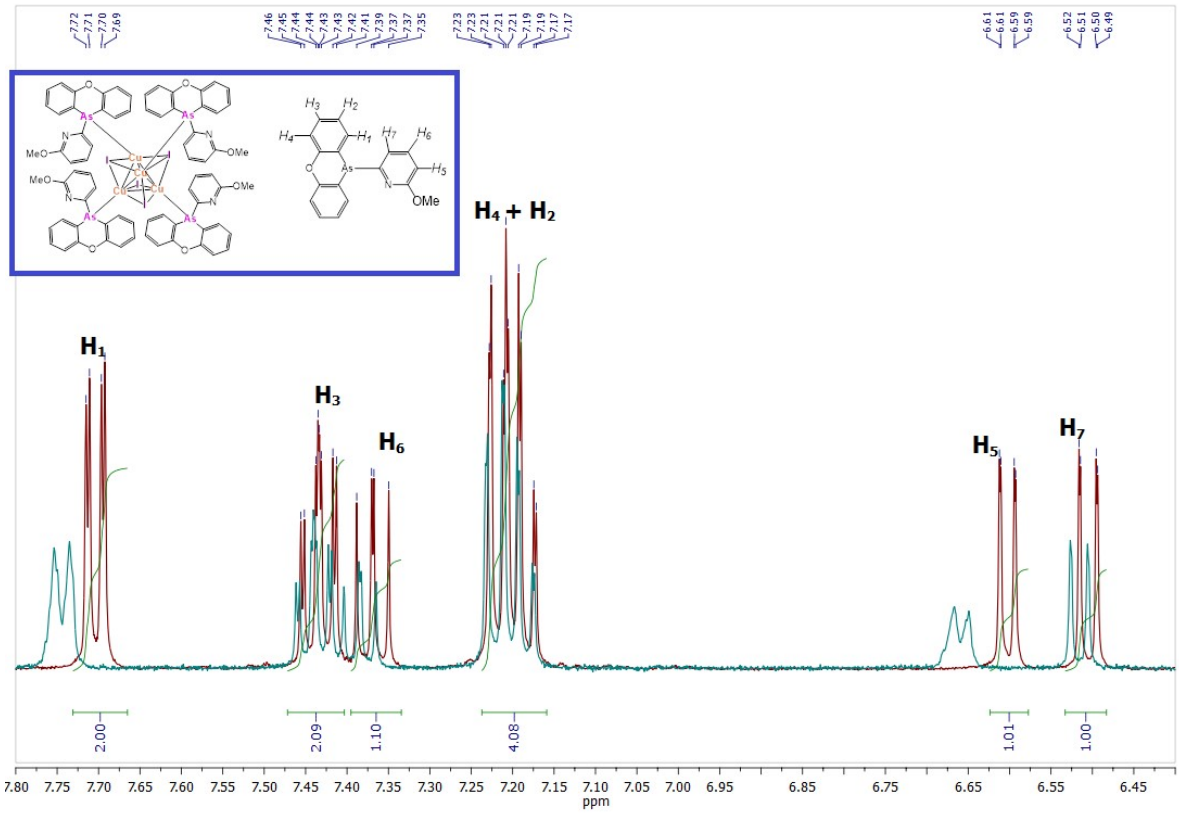

Figure S3. Comparison of ^{1}H NMR spectra for ligand **3** (red line) and complex **7** (green line) measured in CD_3CN (the range from 6.40 to 7.80 ppm is shown). The integrated intensities of NMR signals are given for red spectrum.

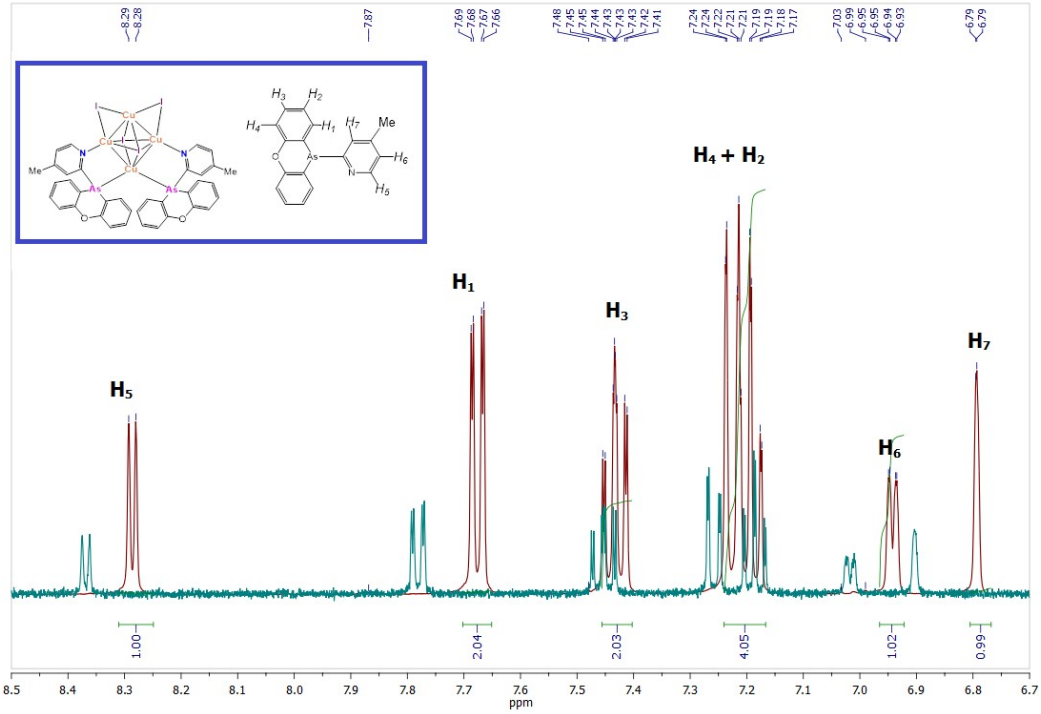

Figure S4. Comparison of ^{1}H NMR spectra for ligand **4** (red line) and complex **8** (green line) measured in CD_3CN (the range from 6.40 to 7.80 ppm is shown). The integrated intensities of NMR signals are given for red spectrum.

2. Single-crystal and powder X-ray diffraction data

Table S1. Crystal data and refinement details for ligands **2**–**4**.

	2	**3**	**4**
empirical formula	C18 H14 As N O	C18 H14 As N O2	C18 H14 As N O
fw	335.22	351.22	335.22
temp.	130	106	130
cryst syst	orthorhombic	monoclinic	monoclinic
space group	*P*na21	*P*21/n	*P*21/n
a (Å)	20.8156(7)	13.8229(10)	11.7742(2)
b (Å)	11.5695(4)	5.9104(4)	18.4805(2)
c (Å)	6.0573(2)	18.3375(13)	13.5881(2)
α(deg)	90	90	90
β(deg)	90	98.575(3)	90.270(1)
γ (deg)	90	90	90
vol ($Å^3$)	1458.76(9)	1481.41(18)	2956.64(7)
Z	4	4	8
density (calcd) (Mg/m^3)	1.526	1.575	1.506
Abs.coeff (mm^{-1})	2.327	2.301	2.297
F(000)	680	712	1360
cryst size (mm^3)	0.05 x 0.10 x 0.60	0.05 x 0.05 x 0.09	0.20 x 0.30 x 0.40
θ range (deg)	2.0, 32.6	1.7, 29.0	1.9, 32.4
index ranges	-30: 31; -16: 15; -9: 9	-18: 18 ; -8: 8 ; -25: 25	-17: 16; -26: 27; -20: 19
reflns collected	13757	67222	44419
independent (R_{int})	4854, 0.050	3935, 0.045	9928, 0.037
data/restraints/parameters	4854, 1, 191	3935, 0, 200	9928, 0, 381
final R indices			
R_1	0.0439	0.0264	0.0329
wR_2	0.0958	0.0721	0.0733
R indices (all data)			
R_1	0.0612	0.0270	0.0507
wR_2	0.1067	0.0726	0.0813
goodness-of-fit on F_2	1.03	1.14	1.05
largest difference peak and hole (e $Å^{-3}$)	0.75, -0.63	1.01, -0.34	0.49, -0.57

Table S2. Crystal data and refinement details for Cu(I) complexes **5**–**8**.

	5	**6**	**6**	**7a**	**8**
measurement temperature (K)	293	130	298	100	293
empirical formula	C68 H48 As4 Cu4 I4 N4 O4	C36 H28 As2 Cu4 I4 N2 O2	C36 H28 As2 Cu4 I4 N2 O2	C56 H45 As3 Cu4 I4 N4 O6	C36 H28 As2 Cu4 I4 N2 O2
fw	2046.58	1432.20	1432.24	1856.52	1432.25
cryst syst	triclinic	triclinic	triclinic	monoclinic	triclinic
space group	*P*-1	*P*-1	*P*-1	*P*21/c	*P*-1
a (Å)	10.1142(18)	10.0169(2)	10.0801(17)	21.9973(18)	12.740(3)
b (Å)	11.804(2)	10.2066(2)	10.3208(18)	16.6381(12)	12.961(3)
c (Å)	14.647(3)	10.8297(2)	10.9161(19)	17.2785(13)	14.868(3)
α(deg)	81.337(10)	102.188(2)	103.093(7)	90	117.28(3)
β(deg)	86.102(10)	100.864(2)	100.312(7)	109.356(3)	110.95(3)
γ (deg)	70.406(9)	110.067(2)	109.725(6)	90	90.70(3)
vol ($Å^3$)	1628.3(5)	974.64(4)	1000.0(3)	5966.4(8)	1991.4(12)
Z	1	1	1	4	2
density (calcd) (Mg/m^3)	2.087	2.440	2.378	2.067	2.389
Abs.coeff (mm^{-1})	5.253	7.040	6.862	5.179	6.891
F(000)	976	668	668	3536	1336
cryst size (mm^3)	0.06 x 0.11 x 0.21	0.12 x 0.23 x 0.37	0.20 x 0.25 x 0.35	0.06 x 0.12 x 0.19	0.05 x 0.12 x 0.23
θ range (deg)	1.4, 27.0	2.0, 35.7	2.2, 36.2	1.6, 30.6	1.7, 27.0
index ranges	-12: 12; -15: 14; -18: 18	-16: 15; -16: 16; -17: 17	-16: 16; -16: 16; -18: 18	-31: 31; -23: 23; -24: 24	-16: 14 ; -16: 14 ; 0: 18
reflns collected	37415	34231	84543	236865	14251
independent (R_{int})	7046, 0.091	8651, 0.023	9081, 0.056	18284, 0.096	14251, 0.000
data/restraints/parameters	7046, 0, 397	8651, 0, 227	9081, 0, 227	18284, 0, 698	14251, 0, 464
final R indices					
R_1	0.0568	0.0249	0.0314	0.0793	0.0474
wR_2	0.1605	0.0570	0.1099	0.2119	0.1105
R indices (all data)					
R_1	0.0878	0.0287	0.0372	0.0875	0.0547
wR_2	0.2190	0.0586	0.1144	0.2153	0.1142
goodness-of-fit on F_2	1.09	1.05	0.89	1.20	1.08
largest difference peak and hole (e $Å^{-3}$)	1.80, -2.55	0.54, -1.31	1.36, -1.23	4.78, -1.65	3.01, -3.45

Table S3. Selected distances (in Å) and angles (°) between the atoms of ligands **2**–**4**.

Structural parameters / **R** at the arsenic atom	**2**	**3**	**4**	
			A	***B***
	6-MePy	**6-(MeO)Py**	**4-MePy**	
As1…$P_{C1C6C7C12}$	0.522	0.412	0.293	0.367
O1…$P_{C1C6C7C12}$	0.292	0.271	0.208	0.241
O1-As1-C_{Ar}	81.64	85.49	90.01	86.59
As1…C13	1.985	1.968	1.970	1.965
∠C13-As1-C1	98.49	99.02	96.70	94.78
∠C13-As1-C12	95.95	96.14	98.77	99.48
∠C1-As1-C12	92.99	93.73	94.75	94.59
Σ	287.43	288.89	290.22	288.85
∠C6-O1-C7	121.33	122.21	123.54	122.82
∠$P_{C1C2C3C4C5C6}$-$P_{C7C8C9C10C11C12}$	27.35	25.41	18.18	21.15
∠$P_{C1C6C7C12}$-$P_{C13C14C15C16C17C18}$	80.12	85.25	89.38	84.30
∠O1-As1-C13-C14	41.43	55.21	47.87	63.62

Table S4. Selected interatomic distances (in Å) and angles (in °) in complex **5**.

structural parameters	**5**
Cu1-Cu2	2.696(1)
Cu1-Cu1’	2.797(2)
Cu1···Cu2’	4.538(2)
Cu1-I2	2.638(1)
Cu2-I2	2.660(1)
Cu1-I1	2.666(1)
Cu1-I1’	2.672(1)
Cu2-I1	2.678(1)
Cu2-As3	2.331(2)
Cu1-N4	2.083(9)
Cu2-N3	2.011(8)
Cu-Cu-Cu’	111.44
Cu-N-As-Cu’	0.65

Table S5. Selected interatomic distances (in Å) and angles (in °) in complex **6**.

structural parameters	**6**	
measurement temperature	298 K	130 K
Cu1-Cu2	2.7018(6)	2.6761(4)
Cu1-Cu1’	2.7437(6)	2.7250(4)
Cu1···Cu2’	2.9801(7)	2.9674(4)
Cu1-I2	2.6761(6)	2.6743(3)
Cu2-I2	2.4980(5)	2.4975(4)
Cu1-I1	2.7381(6)	2.7176(4)
Cu1-I1	2.6701(6)	2.6611(3)
Cu2-I1	2.6426(6)	2.6354(4)
Cu1-As1	2.3823(5)	2.3746(4)
Cu2-N1	1.988(2)	1.982(2)
Cu-Cu-Cu’	66.35	66.64
Cu-N-As-Cu’	27.28	27.35

Table S6. Selected interatomic distances (in Å) in complex **7**.

structural parameters	**7**
Cu2-Cu3	2.692(2)
Cu1-Cu2	2.676(2)
Cu1-Cu3	2.816(2)
Cu3-Cu4	2.666(2)
Cu1-Cu4	2.732(2)
Cu2-Cu4	2.711(1)
Cu1-I1	2.671(1)
Cu2-I1	2.696(2)
Cu3-I1	2.689(1)
Cu2-I2	2.663(1)
Cu3-I2	2.656(1)
Cu4-I2	2.700(1)
Cu1-I3	2.650(1)
Cu3-I3	2.681(1)
Cu4-I3	2.696(2)
Cu1-I4	2.690(2)
Cu3-I4	2.662(1)
Cu4-I4	2.681(1)
Cu2-As3	2.351(1)
Cu3-As2	2.353(2)
Cu4-As1	2.353(1)
Cu1-N60	1.990(8)

Table S7. Selected interatomic distances (in Å) and angles (in °) in complex **8**.

Structural parameters	Complex **8**
Cu3-Cu4	2.522(2)
Cu1-Cu4	2.726(3)
Cu1-Cu2	2.747(2)
Cu2-Cu3	2.589 (2)
Cu4-I4	2.634(2)
Cu3-I4	2.519(2)
Cu2-I3	2.660(2)
Cu3-I3	2.479(1)
Cu4-I2	2.770(2)
Cu3-I2	3.300(1)
Cu2-I2	2.785(2)
Cu1-I2	2.642(2)
Cu1-I1	2.623(2)
Cu2-I1	2.787 (2)
Cu3-I1	2.775 (2)
Cu4-I1	2.819(2)
Cu1-As1	2.347(2)
Cu4-N1	2.032(9)
Cu1-As2	2.342(2)
Cu2-N2	2.026(1)
Cu2-N2-As2-Cu1	7.88(3)
Cu4-N1-As1-Cu1	9.38(3)

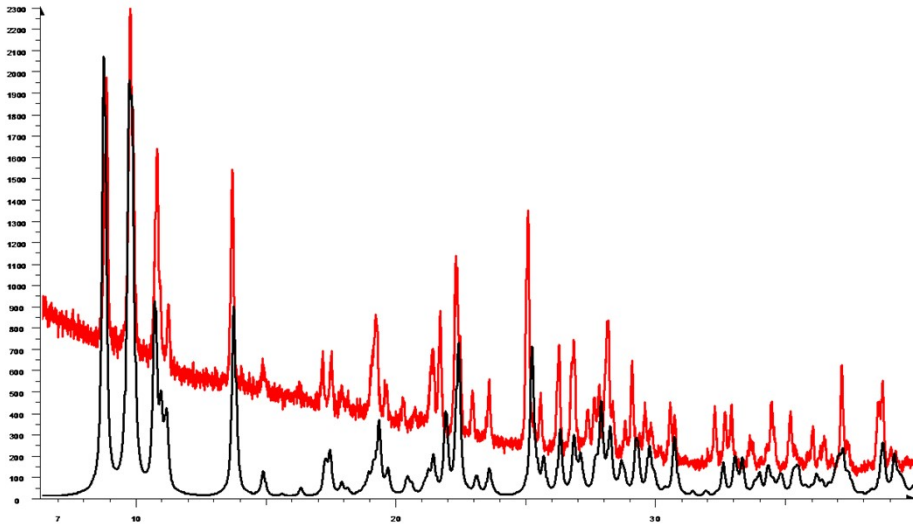

Figure S5. The simulated powder diffractogram (black line) calculated from the single-crystal X-ray data for **5** and the experimental powder diffractogram (red line) of the dried powder sample.

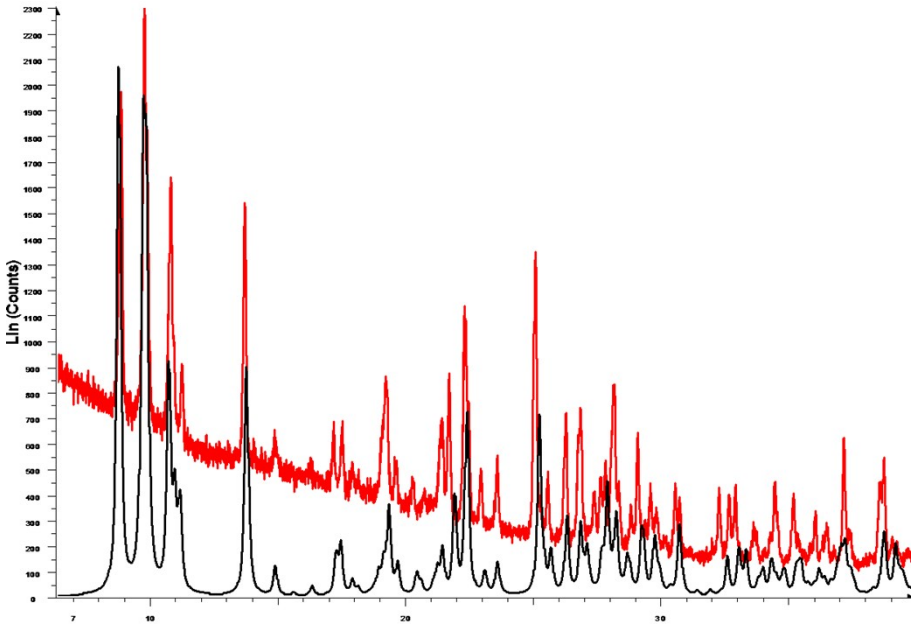

Figure S6. The simulated powder diffractogram (black line) calculated from the single-crystal X-ray data for **6** and the experimental powder diffractogram (red line) of the dried powder sample.

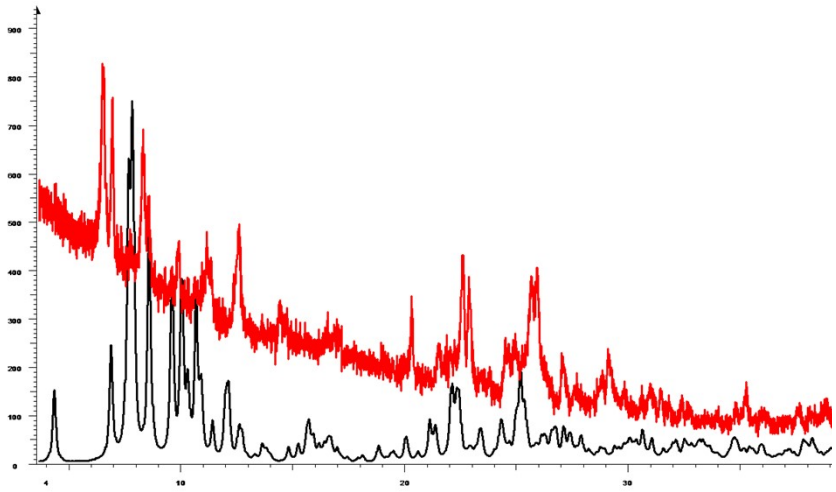

Figure S7. The simulated powder diffractogram (black line) calculated from the single-crystal X-ray data for **7** and the experimental powder diffractogram (red line) of the dried powder sample.

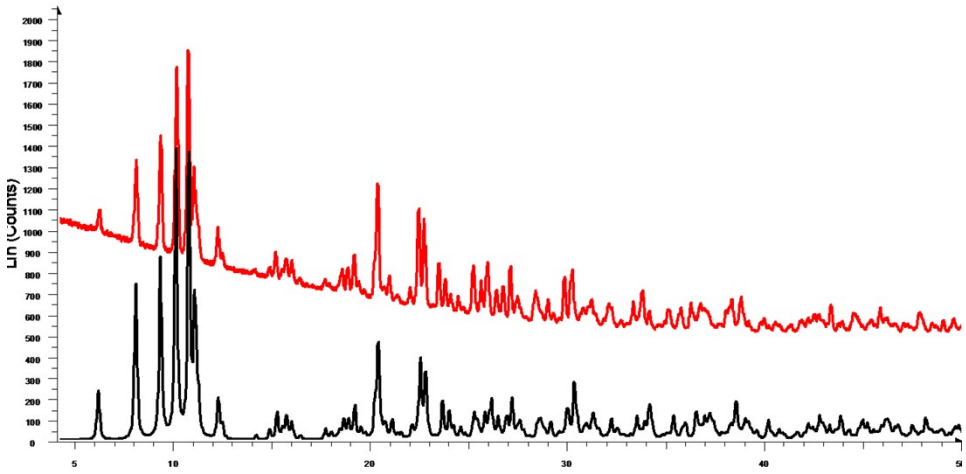

Figure S8. The simulated powder diffractogram (black line) calculated from the single-crystal X-ray data for **8** and the experimental powder diffractogram (red line) of the dried powder sample.

3. Photophysical properties

Experimental data

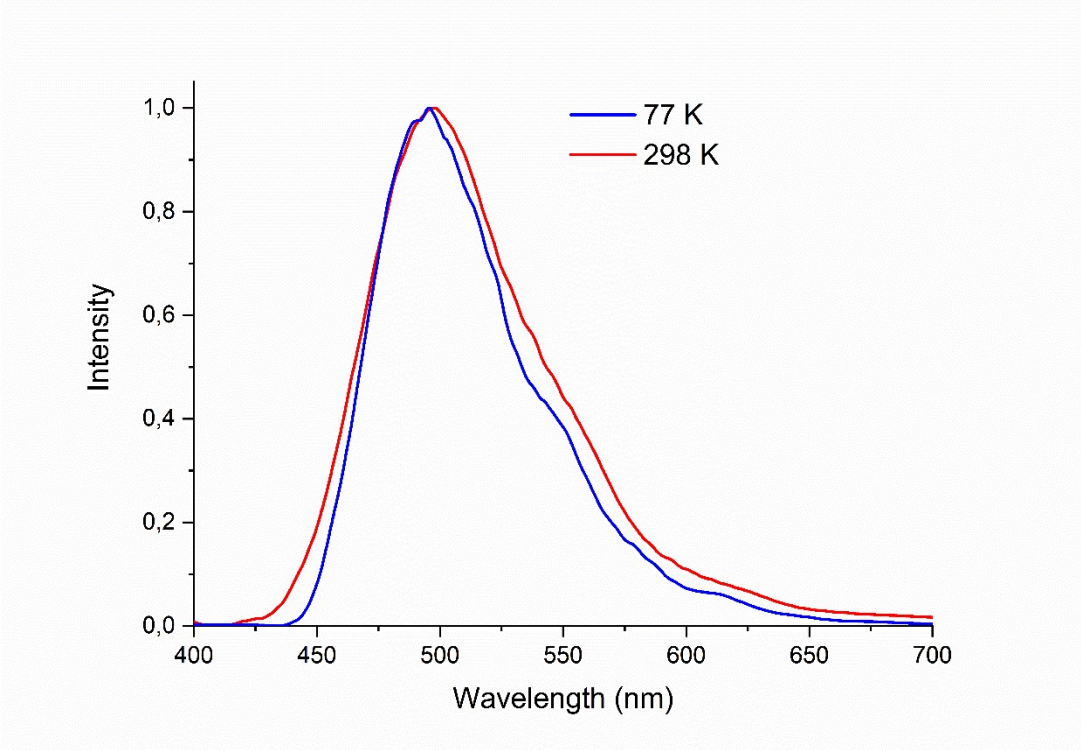

Figure S9. The solid-state emission spectra of complex **5** at 298 and 77 K.

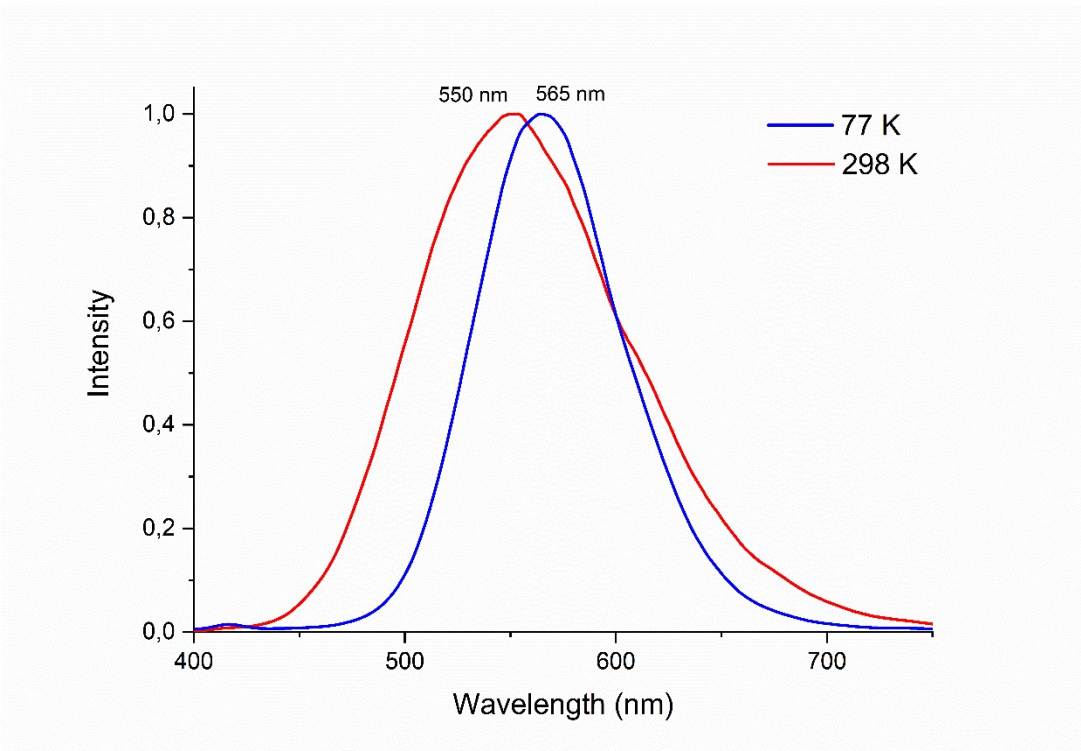

Figure S10. The solid-state emission spectra of complex **7** at 298 and 77 K.

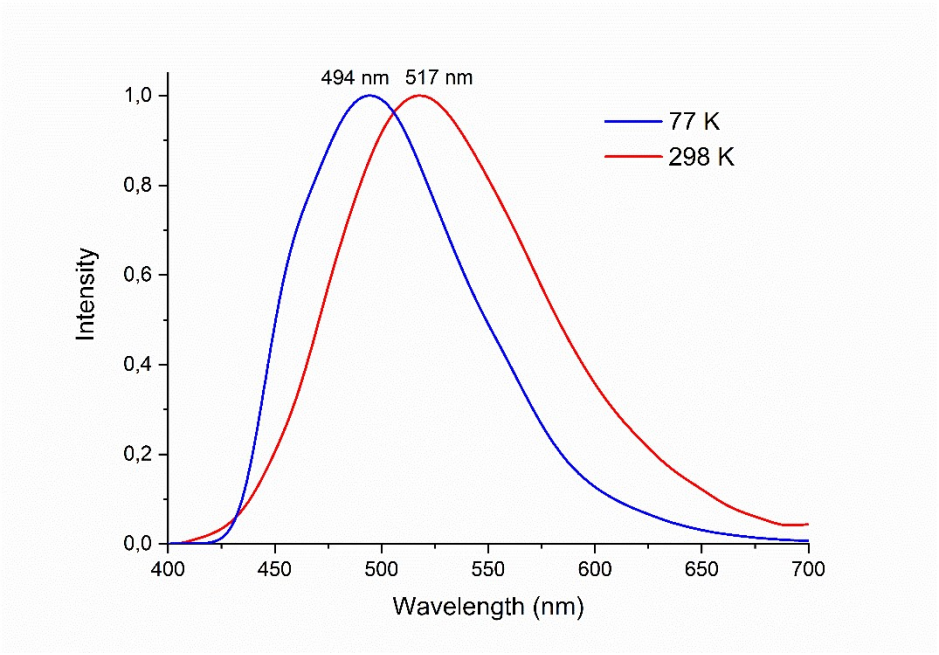

Figure S11. The solid-state emission spectra of complex **8** at 298 and 77 K.

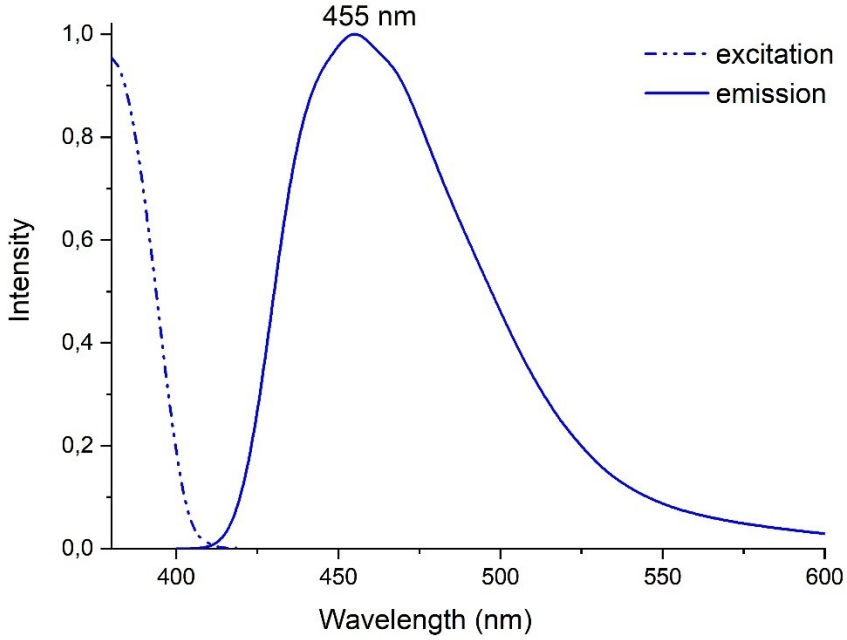

Figure S12. The solid-state excitation and emission spectra of complex **6** at 77 K.

DFT-computed data

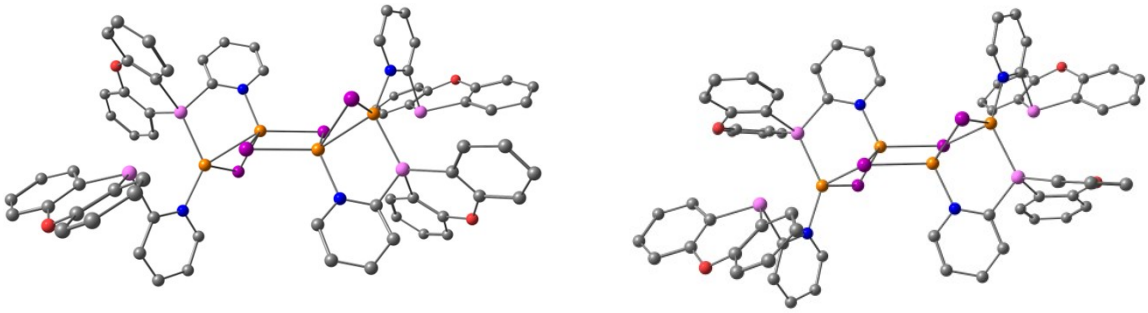

Figure S12. The optimized structures for the singlet ground state S_0 (*left*) and the lowest triplet state T_1 obtained with accounting for the C_i symmetry found in the solid state (*right*) (complex **5**).

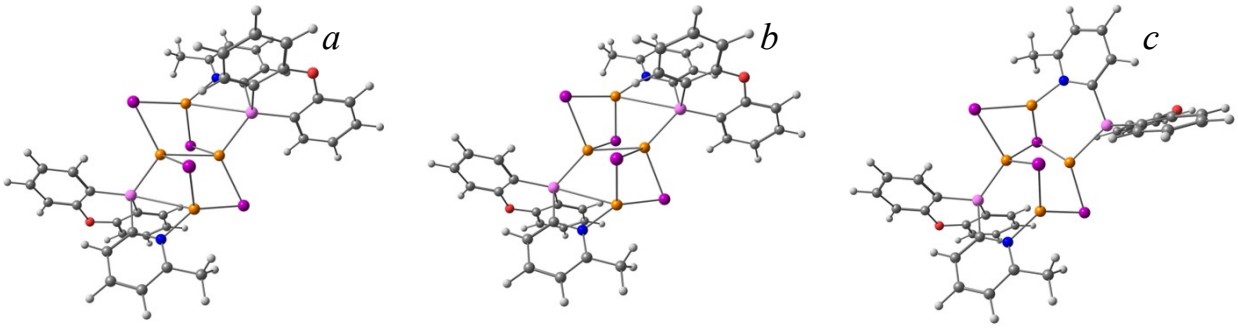

Figure S13. The optimized structures for the singlet ground state S_0 (*a*) and the lowest triplet state T_1 obtained with (*b*) and without (*c*) accounting for the C_i symmetry found in the solid state (complex **6**).

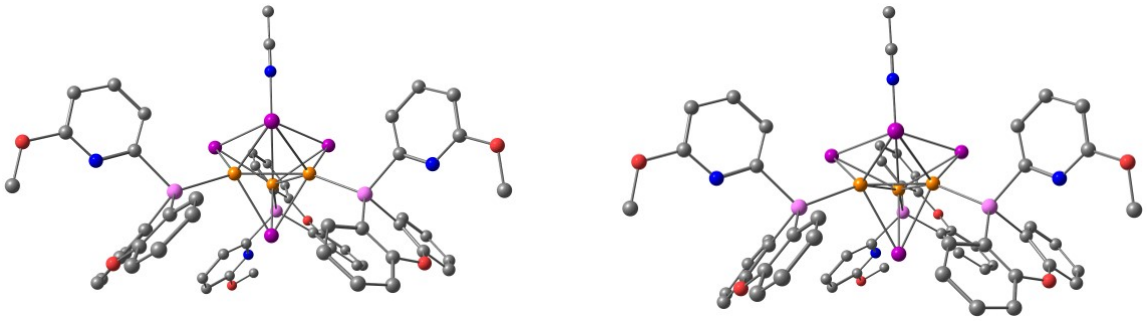

Figure S14. The optimized structures for the singlet ground state S_0 (*left*) and the lowest triplet state T_1 obtained with freezing the torsion angles within the cubane core (*right*) (complex **7**).

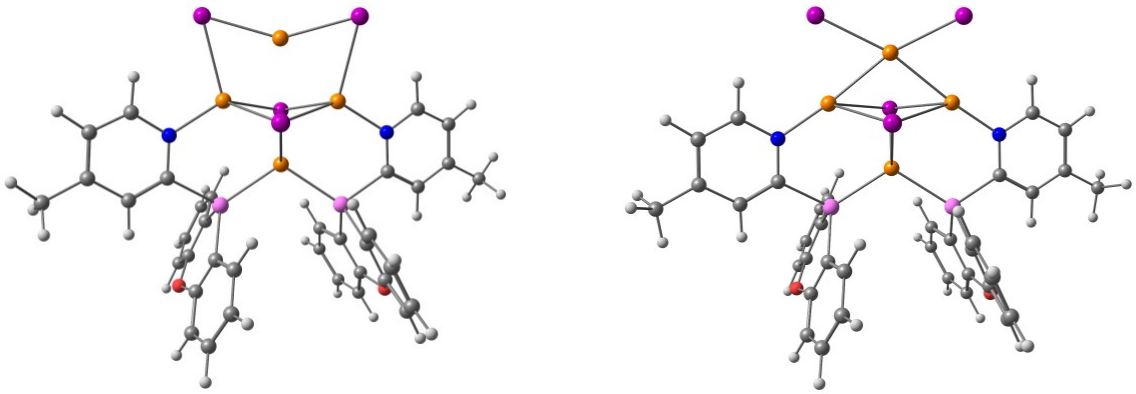

Figure S15. The optimized structures for the singlet ground state S_0 (*left*) and the lowest triplet state T_1 obtained with accounting for the C_2 symmetry found in the solid state (*right*) (complex **8**).

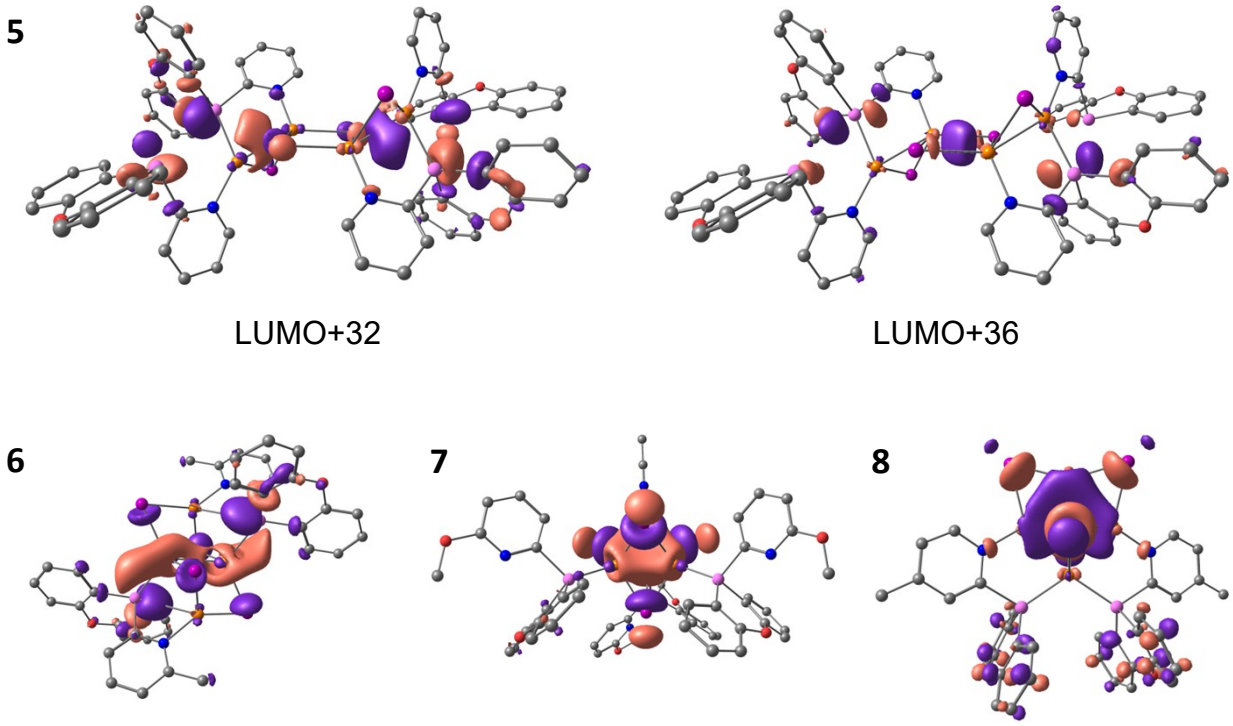

Figure S16. The core-based unoccupied MOs of the singlet ground state calculated at the equilibrium S_0 geometry (complexes **5**–**8**).

4. A collection of the Cu···Cu distance for different Cu_4I_4 tetramers

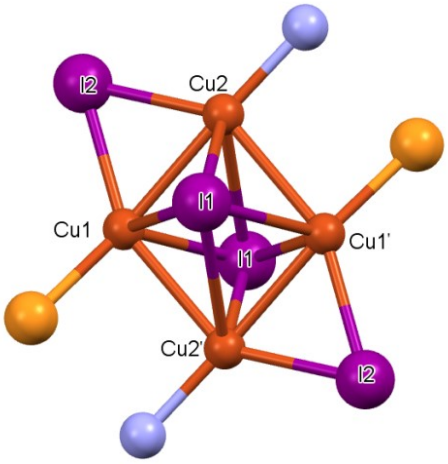

Table S8. Selected bond lengths (Å) for octahedral Cu(I) complexes in the Cambridge Structural Database.

CCDC Identifier	*Ligand type*	*Ligand*	*Cu1–Cu2, Å*	*Cu1···Cu2', Å*	*Cu1-Cu2-Cu1', °*	*Cu2-Cu1'-Cu2', °*	*Ref.*
FALXIZ01	N	quinoline	2.874 2.549	3.453 3.453	81.8	86.6	[S1]
IVAHIZ	N	1-(2-(3,5-dimethyl-1H-pyrazol-1-yl)ethyl)-2-methyl-1,2-dicarba-dodecaborane	2.592	2.929	98.1	81.9	[S2]
FICXOH	N,N	5-*t*-butyl-3-(1-methylpyridin-1-ium-4-yl)-1H-pyrazol-1-yl	2.544* 2.549	2.891 2.834	79.2 69.2	100.8 110.8	[S3]
FICXUN01	N,N	3-(1-methylpyridin-1-ium-4-yl)-5-(trifluoromethyl)-1H-pyrazol-1-yl	2.520	2.918	83.3	96.7	[S3]
FICYIC	N,N	3-(1-methylpyridin-1-ium-4-yl)-5-phenyl-1H-pyrazol-1-yl	2.572	2.907	95.7	84.3	[S3]
BEWCAI	P,P	(dicyclohexylphosphino)methane	2.576	3.005	91.3	88.7	[S4]
JODQIE	P,P	tetrakis(4-allyl-2-methoxyphenyl)phenylimidodiphosphite	2.640	2.891	91.8	88.2	[S5]
JODQOK	P,P	tetrakis(2-allylphenyl)phenylimidodiphosphite	2.568	2.833	90.4	89.6	[S5]
QUGRIW	P,P	5-[bis(2,4,6-trimethylphenyl)boranyl]-2-(diphenylphosphino)-1-methyl-1H-imidazole	2.504	2.829	89.7	90.3	[S6]
QUGSET	P,P	2-(diphenylphosphanyl)-1-methyl-1H-imidazole	2.464	2.784	79.2	100.8	[S6]
ZUDNUJ	P,P	μ2-bis(methyl(2,4,6-tri-isopropylphenyl)phosphino)methane)	2.660	2.810	97.1	82.9	[S7]

CCDC Identifier	*Ligand type*	*Ligand*	*Cu1–Cu2, Å*	*Cu1···Cu2', Å*	*Cu1-Cu2-Cu1', °*	*Cu2-Cu1'-Cu2', °*	*Ref.*
IDUKEA	P,N	2-(diphenylphosphanyl)pyridine	2.539	2.705	89.1	90.9	[S8]
RUXNOP	P,N	4-methyl-2-(phospholan-1-yl)pyridine	2.521	2.788	96.7	83.3	[S9]
RUXPEH	P,N	2-(phospholan-1-yl)pyridine	2.555	2.672	96.6	83.4	[S9]
XOMTUQ	P,N	2-(diphenylphosphino)pyridine	2.588** 2.574	2.750 2.699	81.8 83.1	90.8 91.6	[S10]
AKUMIF	P,N	2-(diphenylphosphanyl)-4-methylpyridine	2.540** 2.540	2.760 2.696	93.4 94.9	85.0 86.4	[S11]
AKUMOL	P,N	2-(diphenylphosphanyl)-6-methylpyridine	2.668	2.748	61.8	118.2	[S11]
BETVIJ	P,N	μ-1,3-bis(diphenylmethyl)-5-(pyridin-2-yl)-1,3,5-diazaphosphinane	2.548	2.722	90.4	89.6	[S12]
BETWAC	P,N	μ-1,3-bis(diphenylmethyl)-5-(pyridin-2-yl)-1,3,5-diazaphosphinane, solvate with C_6H_6	2.556	2.896	84.5	95.5	[S12]
BETVOP	P,N	μ-1,3-bis(diphenylmethyl)-5-(pyridin-2-yl)-1,3,5-diazaphosphinane solvate with acetone	2.540	2.712	92.5	87.5	[S12]
BETVUV	P,N	μ-1,3-bis(diphenylmethyl)-5-(pyridin-2-yl)-1,3,5-diazaphosphinane	2.565	2.805	84.2	95.8	[S12]
CUGCEO	P,N	2-(diphenylphosphino)pyridine	2.574** 2.583	2.682 2.750	91.9 90.5	82.2 80.7	[S13]
HATSIG	P,N	2-((diphenylphosphino)methyl)pyridine	2.525	2.942	90.8	89.2	[S14]
HATSOM	P,N	2-((di-t-butylphosphino)methyl)pyridine	2.630	2.839	96.5	83.5	[S14]
HATSUS	P,N	2-((diisopropylphosphino)methyl)pyridine	2.620	2.880	87.1	92.9	[S14]
HATTAZ	P,N	2-((dicyclohexylphosphino)methyl)pyridine	2.574	2.930	92.3	87.7	[S14]
HATTED	P,N	2-((diethylphosphino)methyl)pyridine	2.562	3.035	98.5	81.5	[S14]

* two independent molecules

** Cu_4 is not planar, dihedral angles *Cu1-Cu2-Cu1'-Cu2' are 25.7°, 4.0° and 29.7° for* XOMTUQ, AKUMIF, CUGCEO, respectively.

Table S9. Selected bond lengths (Å) for stair-step complexes in the Cambridge Structural Database.

CCDC Identifier	*Ligand type*	*Ligand*	*Cu···Cu, Å*	*Ref.*
UGALUM	S	3-ethyl-1,3-benzothiazole-2(3H)-thione	3.143 (x2); 3.367	[S15]
KITPEK	N	1,4-bis(pyridin-4-ylmethyl)piperazine	2.719 (x2); 3.145	[S16]
HEQCUE	P	triphenylphosphine	2.770 (x2); 3.435	[S17]
DEDXIW	P	4-(diphenylphosphanyl)benzoic acid	2.719 (x2); 3.196	[S18]
DEFKUX	P	triphenylphosphine	2.815 (x2); 3.489	[S18]
IGIJIT	P	triphenylphosphine	2.771 (x2); 3.424	[S19]
MARDER	N^N	1,3-bis((2-methyl-1H-imidazol-1-yl)methyl)benzene	2.708 (x2); 2.889	[S20]
MOFVEK	P^P	1,1'-bis(di-t-butylphosphanyl)ferrocene	2.731 3.912 2.734	[S21]
XIVHER	N, N^N	acetonitrile / 3,7-di(pyridin-3-yl)-1,5,3,7-dioxadiazocane	2.747 (x2); 3.084	[S22]
YOQXOT	N, N^N	acetonitrile / 2,2'-(1,4-phenylenebis(methylenesulfanediyl))bis(5-methyl-1,3,4-thiadiazole	2.817 (x2); 2.621	[S23]
EPUNAH	N, P^N	acetonitrile / N-[(diphenylphosphino)methyl]pyrimidin-2-amine	2.828 (x2); 3.474	[S24]
YUMCAN	P, P^N	2,2',2''-[phosphanetriyltri(ethane-2,1-diyl)]tripyridine	3.392 (x2); 2.774	[S25]
UQOVEE	N, S^N	2-(ethylsulfanyl)-1,3-benzothiazole	3.168 (x2); 3.567	[S26]
PIVQES	P, P^N	2-(diphenylphosphino)-5-phenyl-1,3,4-oxadiazole	2.790 (x2); 3.185	[S27]
PIVQIW	P, P^N	2-(diphenylphosphino)-5-phenyl-1,3,4-oxadiazole	2.793 (x2); 3.077	[S27]
PIVQUI	P, P^N	2-(diphenylphosphino)-5-phenyl-1,3,4-thiadiazole	2.702 (x2); 2.898	[S27]
AXAGUE	N^N^S	6,6'-bis[(benzylsulfanyl)methyl]-2,2'-bipyridine	2.692 (x2); 2.981	[S28]
SADYED01	N^S^N	2,2'-disulfanediyldipyridine	2.668 (x2); 2.924	[S29]
GUPMAH	N^N^N	2-((4-((benzylsulfanyl)methyl)-1H-1,2,3-triazol-1-yl)methyl)pyridine	2.615 (x2); 2.783	[S30]
YUSCAR	N^N^N	4,4'-(1,2-phenylene)bis(1-benzyl-1H-1,2,3-triazole	2.631 (x2); 2.746	[S31]

CCDC Identifier	Ligand type	Ligand	Cu···Cu, Å	Ref.
YUSCIZ	N^N^N	4,4'-(4,5-difluoro-1,2-phenylene)bis(1-benzyl-1H-1,2,3-triazole	2.644 (x2); 2.740	[S31]
DOVPAH	N^N^N	2-(1H-1,2,3-triazol-1-ylmethyl)quinoline	2.652 (x2); 2.860	[S32]
DOVPEL	N^N^N	2-((4-propyl-1H-1,2,3-triazol-1-yl)methyl)quinoline	2.670 (x2); 2.992	[S32]
DOVPIP	N^N^N	2-((4-n-butyl-1H-1,2,3-triazol-1-yl)methyl)quinoline	2.707 (x2); 3.072	[S32]
DOVPOV	N^N^N	2-((4-isobutyl-1H-1,2,3-triazol-1-yl)methyl)quinoline	2.597 (x2); 3.001	[S32]
DOVPUB	N^N^N	(1-(quinolin-2-ylmethyl)-1H-1,2,3-triazol-4-yl)methanol	2.639 (x2); 2.953	[S32]
TUGPAP	N^N^N	bis(μ-3,3'-(ethane-1,2-diyl)bis(4,4,5-trimethyl-4H-pyrazole)	2.777 (x2); 2.680	[S33]
ZUGHAM	N^N^N	5-propyl-3-(pyridin-2-ylmethyl)-1H-1,2,3-triazole-1,2(3H)-diyl	2.676 (x2); 2.854	[S34]
ZUGHAM	N^N^N	propane-1,3-diylbis(1-((2-pyridyl)methyl)-1,2,3-triazole-4,2,3(3H)-triyl	2.641; 2,635; 2.969	[S34]
ZUGHIU	N^N^N	butane-1,4-diylbis(1-((2-pyridyl)methyl)-1,2,3-triazole-4,2,3(3H)-triyl	2.642 (x2); 2.706	[S34]

References

[S1] S. Wang, E. E. Morgan, S. Panuganti, L. Mao, P. Vishnoi, G. Wu, Q. Liu, M. G. Kanatzidis, R. D. Schaller, R. Seshadri, *Chem. Mater.* **2022**, *34*, 3206–3216.

[S2] J. Soldevila-Sanmartín, E. Ruiz, D. Choquesillo-Lazarte, M. E. Light, C. Viñas, F. Teixidor, R. Núñez, J. Pons, J. G. Planas, *J. Mater. Chem. C* **2021**, *9*, 7643–7657.

[S3] Y. D. Yu, L. Bin Meng, Q. C. Chen, G. H. Chen, X. C. Huang, *New J. Chem.* **2018**, *42*, 8426–8437.

[S4] W. F. Fu, X. Gan, C. M. Che, Q. Y. Cao, Z. Y. Zhou, N. Nian-Yong Zhu, *Chem. – A Eur. J.* **2004**, *10*, 2228–2236.

[S5] S. Naik, J. T. Mague, M. S. Balakrishna, *Inorg. Chem.* **2014**, *53*, 3864–3873.

[S6] I. Avinash, S. Parveen, G. Anantharaman, *Inorg. Chem.* **2020**, *59*, 5646–5661.

[S7] E. W. Emerson, M. F. Cain, M. D. Sanderson, C. B. Knarr, D. S. Glueck, J. C. Ahern, H. E. Patterson, A. L. Rheingold, *Inorganica Chim. Acta* **2015**, *427*, 168–172.

[S8] A. Neshat, R. Babadi, P. Mastrorilli, S. Todisco, F. Molani, *Polyhedron* **2018**, *154*, 217–228.

[S9] E. I. Musina, A. V. Shamsieva, I. D. Strelnik, T. P. Gerasimova, D. B. Krivolapov, I. E. Kolesnikov, E. V. Grachova, S. P. Tunik, C. Bannwarth, S. Grimme, S. A. Katsyuba, A. A. Karasik, O. G. Sinyashin, *Dalton Trans.* **2016**, *45*, 2250–2260.

[S10] L. Maini, P. P. Mazzeo, F. Farinella, V. Fattori, D. Braga, *Faraday Discuss.* **2014**, *170*, 93–107.

[S11] P. Boden, P. Di Martino-Fumo, J. M. Busch, F. R. Rehak, S. Steiger, O. Fuhr, M. Nieger, D. Volz, W. Klopper, S. Bräse, M. Gerhards, *Chem. – A Eur. J.* **2021**, *27*, 5439–5452.

[S12] I. Strelnik, A. Shamsieva, K. Akhmadgaleev, T. Gerasimova, I. Dayanova, I. Kolesnikov, R. Fayzullin, D. Islamov, E. Musina, A. Karasik, O. Sinyashin, *Chem. – A Eur. J.* **2023**, *29*, e202202864.

[S13] K. Chen, J. Shearer, V. J. Catalano, *Inorg. Chem.* **2015**, *54*, 6245–6256.

[S14] Z. Liu, P. I. Djurovich, M. T. Whited, M. E. Thompson, *Inorg. Chem.* **2012**, *51*, 230–236.

[S15] G. N. Liu, R. Y. Zhao, R. D. Xu, X. Zhang, X. N. Tang, Q. J. Dan, Y. W. Wei, Y. Y. Tu, Q. B. Bo, C. Li, *Cryst. Growth Des.* **2018**, *18*, 5441–5448.

[S16] S. Yuan, S. S. Liu, D. Sun, *CrystEngComm.* **2014**, *16*, 1927–1933.

[S17] Y. Xu, K. Shen, S. Mao, X. Shi, H. Wu, X. Fan, *Appl Organometal Chem.* **2018**, *32*, 4041.

[S18] B. Huitorel, H. El Moll, M. Cordier, A. Fargues, A. Garcia, F. Massuyeau, C. Martineau-corcos, T. Gacoin, S. Perruchas, *Inorg. Chem.* **2017**, *56*, 12379–12388.

[S19] Q. Benito, X. F. Le Goff, G. Nocton, A. Fargues, A. Garcia, A. Berhault, S. Kahlal, J. Y. Saillard, C. Martineau, J. Trébosc, T. Gacoin, J. P. Boilot, S. Perruchas, *Inorg. Chem.* **2015**, *54*, 4483–4494.

[S20] R. Y. Wang, X. Zhang, Q. F. Yang, Q. S. Huo, J. H. Yu, J. N. Xu, J. Q. Xu, *J. Solid State Chem.* **2017**, *251*, 176–185.

[S21] M. Trivedi, G. Singh, A. Kumar, N. P. Rath, *Dalton Trans.* **2014**, *43*, 13620–13629.

[S22] L. Li, H. Y. Li, Z. G. Ren, J. P. Lang, *Eur. J. Inorg. Chem.* **2014**, 824–830.

[S23] K. Xue, W. X. Chai, Y. W. Wu, C. Ling, L. Song, *J. Clust. Sci.* **2014**, *25*, 1005–1017.

[S24] S. Kumar, D. Mondal, M. S. Balakrishna, *ACS Omega* **2018**, *3*, 16601–16614.

[S25] A. V. Artem'ev, A. Y. Baranov, M. I. Rakhmanova, S. F. Malysheva, D. G. Samsonenko, *New J. Chem.* **2020**, *44*, 6916–6922.
[S26] G. N. Liu, R. D. Xu, R. Y. Zhao, Y. Sun, Q. B. Bo, Z. Y. Duan, Y. H. Li, Y. Y. Wang, Q. Wu, C. Li, *ACS Sustain. Chem. Eng.* **2019**, *7*, 18863–18873.
[S27] D. M. Zink, T. Baumann, J. Friedrichs, M. Nieger, S. Bräse, *Inorg. Chem.* **2013**, *52*, 13509–13520.
[S28] C. G. Jiang, Y. F. Yuan, X. Y. Meng, K. K. Zhou, G. L. Zhuang, B. Li, T. Zhang, *Dalton Trans.* **2021**, *50*, 9016–9020.
[S29] M. Pan, W. X. Zhou, W. Y. Ma, J. Niu, J. Li, *J. Coord. Chem.* **2014**, *67*, 3176–3187.
[S30] S. Q. Bai, L. Jiang, A. L. Tan, S. C. Yeo, D. J. Young, T. S. Andy Hor, *Inorg. Chem. Front.* **2015**, *2*, 1011–1018.
[S31] G. F. Manbeck, W. W. Brennessel, C. M. Evans, R. Eisenberg, *Inorg. Chem.* **2010**, *49*, 2834–2843.
[S32] S.-Q. Bai, L. Jiang, D. J. Young, T. S. A. Hor, *Dalton Trans.* **2015**, *44*, 6075–6081.
[S33] T. Yoneda, C. Kasai, Y. Manabe, M. Tsurui, Y. Kitagawa, Y. Hasegawa, P. Sarkar, Y. Inokuma, *Chem. - An Asian J.* **2020**, *15*, 601–605.
[S34] S. Q. Bai, L. Jiang, B. Sun, D. J. Young, T. S. A. Hor, *CrystEngComm.* **2015**, *17*, 3305–3311.